11th International Symposium on Turbulence and Shear Flow Phenomena (TSFP11)
Southampton, UK, July 30 to August 2, 2019

SIMILARITY CONSTRAINTS IN DECAYING ISOTROPIC TURBULENCE

Clayton P. Byers
Department of Engineering
Trinity College
Hartford, CT 06106, United States
clayton.byers@trincoll.edu

Jonathan F. MacArt
Center for Exascale Simulation of
Plasma-Coupled Combustion
University of Illinois at Urbana-Champaign
Urbana, IL 61801, United States
jmacart@illinois.edu

Michael E. Mueller
Dept. of Mechanical and Aerospace Engineering
Princeton University
Princeton, NJ 08544, United States
muellerm@princeton.edu

Marcus Hultmark
Dept. of Mechanical and Aerospace Engineering
Princeton University
Princeton, NJ 08544, United States
hultmark@princeton.edu

ABSTRACT

The focus of this study is to analyze the self-similar scaling approach for decaying isotropic turbulence by comparing a Direct Numerical Simulation with theoretical results. Constraints on the similarity solution are used to show that the temporal evolution of the length scale set the exponent of decay, and a functional form for the dissipation scaling parameter is determined without any curve-fitting to the dissipation data. Collapse of the single time, two-point triple-correlations are shown, with the scaling parameter both differing from the classic analysis and being completely determined from the length scale and double-correlation scaling.

BACKGROUND

A statistical understanding of decaying (unforced) isotropic turbulence begins with the scalar equation for the evolution of the two-point correlation function $F(r,t)$ developed by von Kármán & Howarth (1938) as

$$\frac{\partial F}{\partial t} = \frac{1}{r^4}\frac{\partial}{\partial r}\left[r^4\left(K + 2\nu\frac{\partial F}{\partial r}\right)\right], \tag{1}$$

where $F(r,t) = \langle u_1(x,t)u_1(x+r,t)\rangle$ is the two-point double-correlation, the angle brackets $\langle\cdot\rangle$ represent an ensemble average, and $K(r,t) = \langle u_1^2(x,t)u_1(x+r,t)\rangle$ is the two-point triple-correlation, dependent on the spatial separation and time.

Equation 1 is composed of two scalar functions that depend on two scalar variables, so a similarity solution would enable an understanding of the temporal dependence of the appropriate scaling parameters separate from the spatial dependence of the correlation function. The usual approach to validating similarity via experiments involves first measuring fluctuating velocities in grid turbulence at different downstream locations, then invoking Taylor's hypothesis to transform temporal differences to spatial differences. Another methodology for validation is to utilize data from Direct Numerical Simulations (DNS), which provides full resolution of the spatial, temporal, and velocity information within the computation domain.

The experimental analysis of Batchelor & Townsend (1948) and later investigations by Comte-Bellot & Corrsin (1966) tested the theoretical findings of Batchelor & Townsend (1947), in which it was found that the inverse of the double correlation at zero separation, u^{-2}, and the square of the Taylor microscale, $\lambda^2 = 2u^2/\langle du/dx\rangle^2$, scale linearly in time. More recent experimental studies (Antonia *et al.*, 2003; Lavoie *et al.*, 2007) have investigated the transport of structure functions $\langle(\delta q)^2\rangle \equiv \langle(\delta u)^2\rangle + \langle(\delta v)^2\rangle + \langle(\delta w)^2\rangle$ and found agreement with the classical scaling for the Taylor microscale of $\lambda^2 \sim t$, but determined that the decay of u^2 does not approach t^{-1} for finite Reynolds numbers. These findings agree with the studies of George (1992) and George & Wang (2009), which found that $\langle u^2\rangle$ decays as t^n with $n < -1$. Furthermore, George (1992) and George & Wang (2009) relaxed the constraint on the triple correlation scaling parameter, finding that K should be scaled with u^3/Re_λ, where $Re_\lambda = u\lambda/\nu$ is the Taylor-scale Reynolds number and $u = \langle u_1^2\rangle^{1/2}$, which differed from the classic Batchelor & Townsend (1947) scaling of u^3. This updated approach was utilized by Antonia *et al.* (2003) and Lavoie *et al.* (2007) in their study of structure functions and found agreement with the conclusions of George (1992) and George & Wang (2009) for the double and triple correlations.

WHAT WE FIND FROM SIMILARITY

The self-similar forms for the scaling parameters in decaying isotropic turbulence have been derived and discussed in Batchelor & Townsend (1947), George (1992) and Lavoie *et al.* (2007). The two-time solutions from Byers *et al.* (2017) utilized the process outlined in George (1992) and reduce to the subsequent single-time results as a spe-

cial case. Utilizing the notation from Byers *et al.* (2017), the two-point double- and triple-correlations are proposed to have the following similarity forms:

$$F(r,t) = R_s(t)\, f(\eta) \tag{2a}$$

$$K(r,t) = T_s(t)\, k(\eta) \tag{2b}$$

$$\eta = \frac{r}{\delta(t)}, \tag{2c}$$

where $R_s(t)$ and $T_s(t)$ are temporally-dependent dimensional scaling parameters, $f(\eta)$ and $k(\eta)$ are non-dimensional similarity functions, η is a non-dimensional spatial separation between two points x and $x+r$, and $\delta(t)$ is a temporally-evolving length scale.

Substituting equations 2a-2c into equation 1 and rearranging produces the following scaled equation:

$$\left[\frac{\delta^2}{\nu R_s}\frac{dR_s}{dt}\right] f - \left[\frac{\delta}{\nu}\frac{d\delta}{dt}\right]\eta\frac{df}{d\eta} = \left[\frac{\delta T_s}{\nu R_s}\right]\frac{1}{\eta^4}\frac{d}{d\eta}\left(\eta^4 k\right) + [2]\,\frac{1}{\eta^4}\frac{d}{d\eta}\left(\eta^4\frac{df}{d\eta}\right). \tag{3}$$

This form of the Von-Karman-Howarth equation has all the temporally-dependent dimensional terms contained in brackets, while the terms outside are non-dimensional variables and scaling functions. For equilibrium similarity to hold, the bracketed terms must evolve in the same manner or be identically zero, since no term in equation 1 should become more relevant than another throughout the range of equilibrium similarity (George, 1992). The bracketed terms therefore all have the same temporal dependence under this constraint of equilibrium similarity:

$$\left[\frac{\delta^2}{\nu R_s}\frac{dR_s}{dt}\right] \sim \left[\frac{\delta}{\nu}\frac{d\delta}{dt}\right] \sim \left[\frac{\delta T_s}{\nu R_s}\right] \sim [2] = constant, \tag{4}$$

where '$\sim$' is utilized to represent a similar temporal dependence. With equation 4 indicating all bracketed terms are constants, they can be integrated to produce the following functional forms for the scaling parameters:

$$\delta^2 = \lambda^2 = 2A\nu(t-t_0) \tag{5a}$$

$$R_s = u^2 = R_0(t-t_0)^{\frac{B}{2A}} \tag{5b}$$

$$T_s \equiv \frac{u^3}{Re_\lambda} = \frac{C\nu R_0}{\sqrt{2A\nu}}\left(t-t_0\right)^{\frac{B}{2A}-\frac{1}{2}}, \tag{5c}$$

where t_0 and R_0 are constants of integration, and A, B, and C are constants that constrain the similarity behavior of the Von-Karman-Howarth equation. These similarity constraints are defined as:

$$A = \frac{\lambda}{\nu}\frac{d\lambda}{dt}, \quad B = \frac{\lambda^2}{\nu u^2}\frac{du^2}{dt}, \quad C = \frac{\lambda T_s}{\nu u^2}. \tag{6}$$

Note these constraints are exactly those obtained from the similarity analysis in equation 4 with the length scale chosen as the Taylor microscale and the double correlation scale chosen as u^2, while the triple correlation scale T_s has been determined from the scaling analysis and does not have the freedom to be specified independently.

The equilibrium similarity analysis requires that the parameters in equation 6 must be constant for any given Reynolds number. In equation 5c, C is immediately determined from comparing that functional form with the decay functions for both $u^3 = \langle u^2\rangle^{3/2}$ and λ, giving $C = 1$. Note too that equation 5c is not simply the $3/2$ power of u^2 but also contains an explicit Reynolds number dependence, contrasting the classic approach of Batchelor & Townsend (1947) in which it was assumed that $K(r,t)$ is scaled with u^3. The result of this analysis matches the prediction of George (1992) and George & Wang (2009), where their analysis of the spectral equations found a Reynolds number dependence in the spectral transfer scaling parameter, analogous to this triple correlation in the physical domain.

In decaying isotropic turbulence, the dissipation can be related to the kinetic energy of the flow:

$$\frac{d}{dt}\left(\frac{3}{2}u^2\right) = -\varepsilon. \tag{7}$$

Combining equations 5b and 7 results in a dissipation scaling parameter:

$$\varepsilon_s = -\frac{3}{2}\frac{R_0 B}{2A}\left(t-t_0\right)^{\frac{B}{2A}-1}. \tag{8}$$

Note that every term in equation 8 is determined from the previous scaling relations, meaning that the dissipation scaling is uniquely determined from the length scale and double-correlation scaling. The isotropic relation

$$\varepsilon = 30\nu\frac{u^2}{\lambda^2} \tag{9}$$

can be combined with equation 8,

$$-\frac{3}{2}\frac{R_0 B}{2A}\left(t-t_0\right)^{\frac{B}{2A}-1} = 30\nu\frac{R_0(t-t_0)^{\frac{B}{2A}}}{2A\nu(t-t_0)}, \tag{10}$$

which, upon canceling terms, results in a predicted value of $B = -20$. Note the coefficient of 30 in equation 9 is due to the Taylor microscale having a factor of 2 in its definition. This theoretical value of B can further inform the value of A through the power in equation 5b, where $B/2A \to -1$ in the infinite Reynolds number limit. This implies that $A \to 10$ as Re grows infinitely large.

RESULTS AND CONCLUSIONS

Three DNS calculations of decaying isotropic turbulence are performed. The number of grid points $N = 1536^3$ and periodic box size are fixed, while the Reynolds number is varied by changing the initial integral length scale. The initial condition is generated using a synthetic turbulence spectrum (Passot & Pouquet, 1987) and is allowed to decay for approximately two eddy-turnover times before correlation functions are evaluated. That this delay allows for the development of sufficiently-equilibrated turbulence is justified in the next section. The Taylor-scale Reynolds number

Table 1. Parameters extracted from each DNS case.

Case	N	Re_λ	A	B	Sym.
1	1536^3	36.5	7.047	-19.910	$\triangledown$
2	1536^3	41.5	8.194	-19.923	$\diamond$
3	1536^3	55.9	8.412	-19.775	$\triangle$

at the time equilibrium is achieved (A, B become constant) is listed for each case in table 1.

The incompressible Navier-Stokes equations are solved using an energy-conservative, semi-implicit, iterative algorithm for low Mach number flows (Desjardins *et al.*, 2008; MacArt & Mueller, 2016), in which the momentum equation and a Poisson equation for the hydrodynamic pressure are updated using a fractional-step scheme (see Kim & Moin, 1985). Spatial derivatives are obtained using second-order central differences on a staggered grid, in which velocity components are located at cell faces and the pressure is located at cell centers. The grid resolves the initial Kolmogorov scale to within a factor of two, meaning that the spatial resolution of the Kolmogorov scale improves with time. The initial resolution is generally sufficient for DNS of decaying isotropic turbulence (Yeung & Pope, 1989).

Evaluation of the Scaling Parameters

The cases tested are listed in table 1, and it is apparent that $B = -20$ for all flows, while A trends towards 10 as the Reynolds number increases. Figure 1a shows the evaluation of similarity constraints A and B in equation 6, indicating a temporal lag of nearly two eddy turnover times between the start of the simulation and the equilibrium decay where the constraints approach constant values. The scaling functions in equations 5a - 5c as well as equation 8 will then be evaluated only after this equilibrium decay is achieved.

The values for A in each case are then applied to the fits for λ^2, shown in figure 1b. The linear behavior of λ^2 is apparent in each test case, conforming to the predictions from classic results (Batchelor & Townsend, 1947; George, 1992). Note that the higher Reynolds number achieved a better fit between the theory and data, which is likely due to equilibrium conditions holding over longer periods of time.

The decay exponent for u^2, $B/2A$, is then immediately determined, for A has been calculated and it was shown that $B = -20$. This means the decay exponent is not a fitting parameter but instead is uniquely determined by the evolution of the length scale. As shown in table 1, the Reynolds number dependence of A therefore means the decay rate is asymptotically flow independent for high Reynolds numbers at best and not a universal constant, which agrees with the prediction of George (1992). The double-correlation is then shown to follow the functional form of equation 5b in figure 2a. As previously discussed, the triple correlation can immediately be determined by setting $C = 1$, with figure 2a demonstrating the agreement between data and theory. It should not be surprising that the triple scale and equation 5c match so well, since they are both uniquely determined from the Taylor microscale and the double correlation scale.

Additionally, the dissipation scaling is compared to the data in figure 2b. The dissipation was calculated directly from the integrated spectrum, shown in black,

$$\varepsilon = 2\nu \int_0^\infty \tilde{k}^2 E(\tilde{k}) d\tilde{k} \tag{11}$$

where $\tilde{k}$ is the wavenumber and $E(\tilde{k})$ is the scalar energy distribution, found by integrating the Fourier transform of the autocorrelation of u over spherical shells. This is compared to the modeled dissipation

$$\varepsilon = 30\nu \frac{u^2}{\lambda^2} \tag{12}$$

which is shown in red in figure 2b. The agreement with the dissipation scaling of equation 8 is expected, as the equilibrium similarity analysis indicated that the dissipation scaling is a direct result of the length scale and double correlation scale.

Overall, the agreement between the derived scaling parameters and the DNS results demonstrate that the equilibrium similarity analysis is appropriate for determining the similarity forms. In the next section, the double- and triple-correlation functions are analyzed after sufficiently equilibrated turbulence is obtained, indicated as the point in time at which A and B reach approximately constant values. This point appears to be approximately two initial eddy-turnover times.

Collapsing the Double- and Triple-Correlation Functions

The scaling parameters obtained in the previous section are used to collapse the double- and triple-correlation functions after $t/t_s \approx 1.8$. The double correlation, $F(r,t)$, is shown in figure 3a for Case 2, where both the spatial and temporal dependence is apparent. The profiles are scaled by u^2 and λ in figure 3b, which demonstrates the expected spatial and temporal collapse.

Of greater interest and new to these authors is the collapse of the triple correlation from the developed scaling parameter in equation 5c. Measurements of the triple correlation have been shown in Stewart (1951); Stewart & Townsend (1951), who used an analog integrator to extract the measurement. No collapse in the decay was shown, but the scaling also assumed a simple $\left(u^2\right)^{3/2}$ factor. Inspection of equation 5c shows that the exponent will approach $-3/2$ only if $-B/2A \to -1$. The results summarized in table 1 indicate this may occur as the Reynolds number grows infinitely large, as the similarity constraint B should remain a constant -20 while A appears to approach 10 as the Reynolds number increases. This would explain why the triple correlation profiles of Stewart (1951); Stewart & Townsend (1951) did not collapse, since their experiment was not at an infinitely high Re_λ.

Figure 4 shows both the unscaled and scaled $K(r,t)$ for all three cases. Each scaled case collapses to a nearly universal profile in figure 4b, but only within the case. For the increasing Reynolds number, the overall magnitude of the plot is growing. While the intra-case collapse justifies u^3/Re_λ as the appropriate scaling parameter and demonstrates that the evolution of the length scale sets the decay exponent, the inter-case Reynolds number dependence is not explained. It is possible that the similarity constraint C evolves with Reynolds number, just as A does. However,

further investigation is needed to explain what dependence it may have. Since the triple correlation is zero at $r = 0$, there is no straightforward parameter or scale to use in evaluating the growth rate of C with Re_λ.

As a final note, the spreading of the triple-correlation tails observed in figure 4 is likely due to the finite computational domain size. Future work will explore this possibility using similar-Reynolds number DNS data obtained on larger computational domains.

REFERENCES

Antonia, Robert A, Smalley, RJ, Zhou, Tongming, Anselmet, Fabien & Danaila, Luminita 2003 Similarity of energy structure functions in decaying homogeneous isotropic turbulence. *Journal of Fluid Mechanics* **487**, 245–269.

Batchelor, GK & Townsend, AA 1947 Decay of vorticity in isotropic turbulence. In *Proc. R. Soc. Lond. A*, , vol. 190, pp. 534–550. The Royal Society.

Batchelor, GK & Townsend, AA 1948 Decay of isotropic turbulence in the initial period. In *Proceedings of the Royal Society of London A: Mathematical, Physical and Engineering Sciences*, , vol. 193, pp. 539–558. The Royal Society.

Byers, Clayton P, Hultmark, Marcus & George, William K 2017 Two-space, two-time similarity solution for decaying homogeneous turbulence. *Physics of Fluids* **29** (2), 020710.

Comte-Bellot, Genevieve & Corrsin, Stanley 1966 The use of a contraction to improve the isotropy of grid-generated turbulence. *Journal of fluid mechanics* **25** (4), 657–682.

Desjardins, Olivier, Blanquart, Guillaume, Balarac, Guillaume & Pitsch, Heinz 2008 High order conservative finite difference scheme for variable density low mach number turbulent flows. *Journal of Computational Physics* **227** (15), 7125–7159.

George, William K 1992 The decay of homogeneous isotropic turbulence. *Physics of Fluids A: Fluid Dynamics* **4** (7), 1492–1509.

George, William K & Wang, Honglu 2009 The exponential decay of homogeneous turbulence. *Physics of Fluids* **21** (2), 025108.

von Kármán, Theodore & Howarth, Leslie 1938 On the statistical theory of isotropic turbulence. In *Proceedings of the Royal Society of London A: Mathematical, Physical and Engineering Sciences*, , vol. 164, pp. 192–215. The Royal Society.

Kim, John & Moin, Parviz 1985 Application of a fractional-step method to incompressible Navier-Stokes equations. *Journal of Computational Physics* **59** (2), 308–323.

Lavoie, P, Djenidi, L & Antonia, RA 2007 Effects of initial conditions in decaying turbulence generated by passive grids. *Journal of Fluid Mechanics* **585**, 395–420.

MacArt, Jonathan F & Mueller, Michael E 2016 Semi-implicit iterative methods for low mach number turbulent reacting flows: Operator splitting versus approximate factorization. *Journal of Computational Physics* **326**, 569–595.

Passot, Thierry & Pouquet, Annick 1987 Numerical simulation of compressible homogeneous flows in the turbulent regime. *Journal of Fluid Mechanics* **181**, 441–466.

Stewart, RW 1951 Triple velocity correlations in isotropic turbulence. In *Mathematical Proceedings of the Cambridge Philosophical Society*, , vol. 47, pp. 146–157. Cambridge University Press.

Stewart, RW & Townsend, A A 1951 Similarity and self-preservation in isotropic turbulence. *Phil. Trans. R. Soc. Lond. A* **243** (867), 359–386.

Yeung, PK & Pope, SB 1989 Lagrangian statistics from direct numerical simulations of isotropic turbulence. *Journal of Fluid Mechanics* **207**, 531–586.

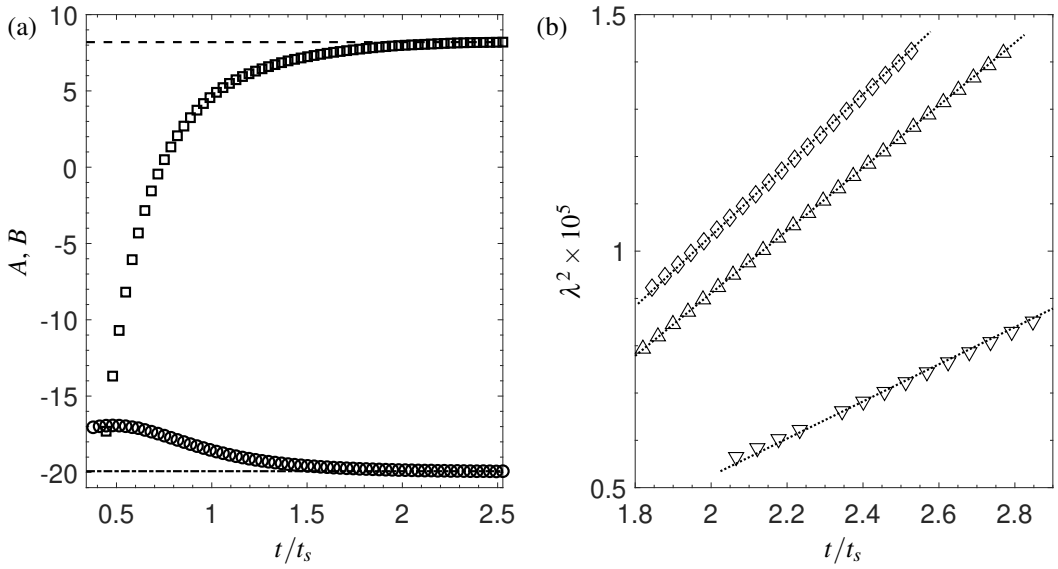

Figure 1. Calculations from equation 6 of the similarity constants A and B shown in □ and ○ symbols, respectively, in (a). Time is non-dimensionalized by initial eddy turnover time $t_s = 3u^2/2\varepsilon$ evaluated at the start of the simulation. Data presented is from case 2. The growth of λ^2 for all DNS cases is shown in (b) for later times when A and B approach a constant value. Equation 5a is shown as a dotted line for each data set.

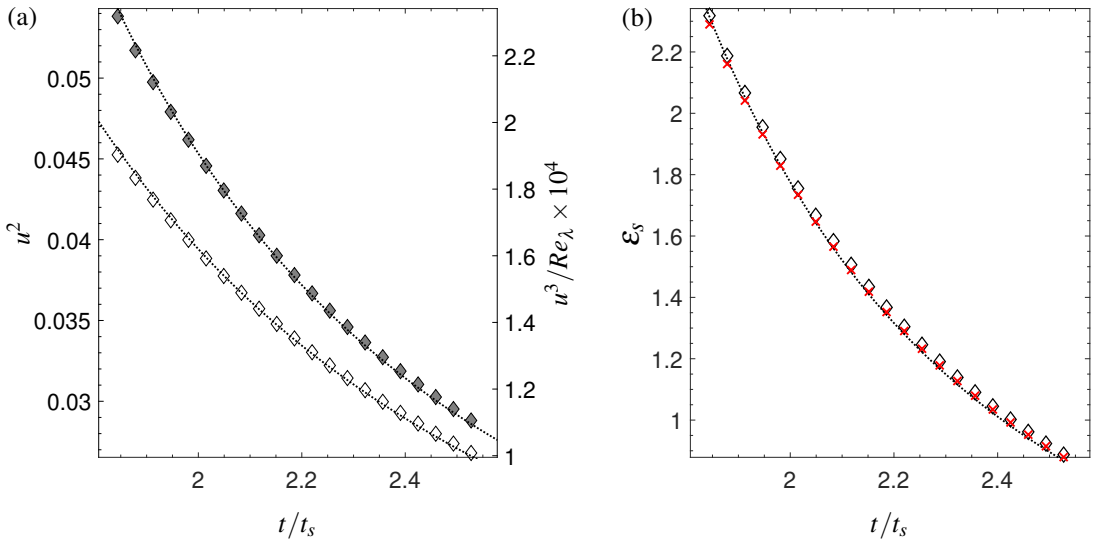

Figure 2. Temporal decay of the double-correlation scale u^2, shown in hollow symbols, and the triple-correlation scale u^3/Re_λ, shown in gray symbols in (a). Dotted lines follow equation 5b for u^2 and 5c for u^3/Re_λ. Dissipation is shown in (b) and plotted with the relation of equation 8 (dotted line). Also shown is the calculated $\varepsilon = 30\nu u^2/\lambda^2$ in red. All data presented is from case 2.

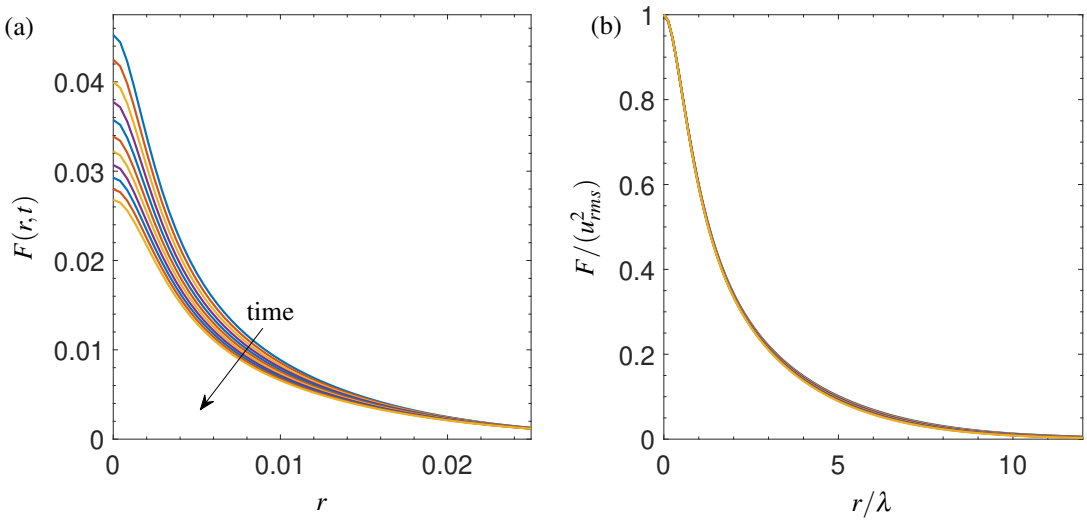

Figure 3. Unscaled (a) and scaled (b) double correlations. Increasing time corresponds to decreasing magnitude in (a), while profiles collapse in (b) under the scaling. All data is Case 2, while Cases 1 and 3 show similar behavior.

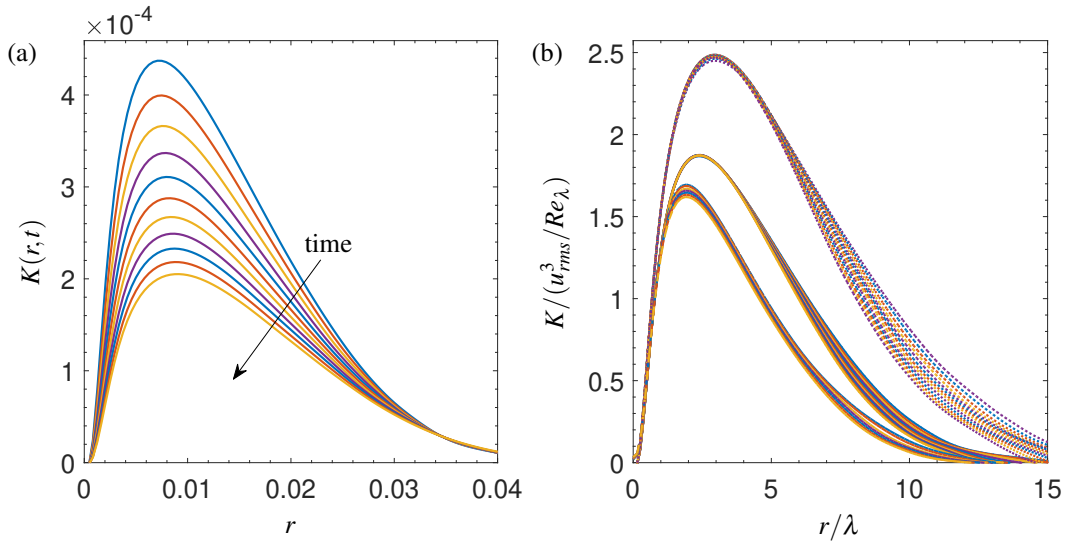

Figure 4. Unscaled (a) and scaled (b) triple correlations. Increasing time corresponds to decreasing magnitude in (a), while profiles collapse in (b) under the scaling, where Case 1 is shown in dashed lines (lowest magnitude), Case 2 in solid, and Case 3 in dotted lines (highest magnitude). The scaling works by accounting for the decreasing Reynolds number in each simulation but not the differences in Reynolds number between cases, which remains a point of ongoing investigation.